Journal of Experimental Botany, Vol. 47, No. 296, pp. 411–420, March 1996

Journal of Experimental Botany

An architectural analysis of the elongation of field-grown sunflower root systems. Elements for modelling the effects of temperature and intercepted radiation

L.A.N. Aguirrezabal[1] and F. Tardieu[2,3]

[1] *Catedra de Fisiologia Vegetal, Facultad de Ciencias Agrarias, Universidad Nacional de Mar del Plata, c.c. 276, 7620 Balcarce, Argentina*

[2] *INRA, Ecophysiologie des Plantes sous Stress Environnementaux, 2, place Viala, F-34060 Montpellier cedex 1, France*

Received 10 May 1995; Accepted 23 November 1995

Abstract

The effects of photosynthetic photon flux density (*PPFD*) and soil temperature on root system elongation rate have been analysed by using an architectural framework. Root elongation rate was analysed by considering three terms, (i) the branch appearance rate, (ii) the individual elongation rates of the taproot and branches and (iii) the proportion of branches which stop elongating. Large ranges of *PPFD* and soil temperature were obtained in a series of field and growth chamber experiments. In the field, the growth of root systems experiencing day-to-day natural fluctuation of *PPFD* and temperature was followed, and some of the plants under study were shaded. In the growth chamber, plants experienced contrasting and constant *PPFD*s and root temperatures. The direct effect of apex temperature on individual root elongation rate was surprisingly low in the range 13–25 °C, except for the first days after germination. Root elongation rate was essentially related to intercepted *PPFD* and to distance to the source, both in the field and in the growth chamber. Branch appearance rate substantially varied among days and environmental conditions. It was essentially linked to taproot elongation rate, as the profile of branch density along the taproot was quite stable. The length of the taproot segment carrying newly appeared branches on a given day was equal to taproot elongation on this day, plus a 'buffering term' which transiently increased if taproot elongation rate slowed down. The proportion of branches which stopped elongating a short distance from the taproot ranged from 50–80% and was, therefore, a major architectural variable, although it is not taken into account in current architectural models. A set of equations accounting for the variabilities in elongation rate, branch appearance rate and proportion of branches which stop elongating, as a function of intercepted *PPFD* and apex temperature is proposed. These equations apply for both field and growth chamber experiments.

Key words: Sunflower, root system, model, temperature, radiation.

Introduction

Temperature and intercepted solar radiation are now currently used for predicting plant phenology and growth in whole-canopy models (e.g. CERES-wheat, Ritchie and Otter 1984; EPIC, Williams *et al.*, 1984, 1989). In these models, prediction applying to roots is usually carried out by considering the elongation of a 'mean' root. Mean elongation rate is calculated as the ratio of carbon flux available for root growth to mean carbon mass per unit root length. Thus, these models do not take into account the fact that elongation of a root system consists of the sum of elongations of roots of different orders, which each have their own elongation rate and elongation duration. On the other hand, architectural models of root systems can predict the branching and elongation of individual roots on a time basis (Lungley, 1973) or a heat unit basis (Porter *et al.*, 1986; Diggle, 1988; Pagès

[3] To whom correspondence should be addressed. Fax: +33 67 52 21 16.

and Aries, 1988), but they have no environmental inputs other than air temperature. Their main application until now has been to compare ideotypes of root systems of different species or cultivars, rather than to predict root growth under the naturally fluctuating environmental conditions observed in the field.

The objective of the work reported here was to use Lungley's (1973) architectural framework in order to analyse the consequences of changes in temperature and intercepted *PPFD* on the growth and architecture of field-grown sunflower root systems. This approach involved (i) assessing Lungley's assumptions for field-grown sunflower, (ii) investigating, among the parameters of Lungley's model, which parameters appreciably vary and which remain stable in a range of contrasting environmental conditions and (iii) getting experimental relationships between parameters of the model and environmental inputs, with a daily timestep. This analysis was carried out in a series of field experiment in two locations, and in a series of growth chamber experiments. Environmental conditions, other than *PPFD* and soil temperature, were kept at a near-optimal level by maintaining adequate levels of water and nutrient concentrations in the soil.

Framework of analysis

Sunflower root systems consist of a taproot, which elongates almost vertically in the soil, and of branches of 1st, 2nd and 3rd order. Since 2nd and 3rd order branches are usually short (Weaver, 1926; Kutschera, 1960), the approach was limited to taproot and 1st order branches. In effect, accumulation of short roots around first order branches causes a high degree of clumping, so that 2nd and 3rd order branches probably have a limited individual contribution to water and nitrogen uptakes in field conditions (Tardieu *et al.*, 1992). In the taproot, cells appear in the zone of division, a few millimetres behind the apex, and elongate at further distance from the apex. The respective lengths of both zones have not been measured in sunflower roots, they are *c.* 3 mm and 10 mm, respectively, in maize seminal roots (Sharp *et al.*, 1988; Fraser *et al.*, 1990). Secondary roots appear acropetally, at *c.* 300 mm behind the tip (Fig. 1a). Material points (Gandar, 1980; Silk, 1992), e.g. points on the taproot where a branch will eventually appear, therefore, flow continuously from the root tip to the ramified zone of the taproot. They cross the elongating zone and then the remaining part of the non-ramified zone. Three variables contribute to the variability in total root elongation on day i: taproot elongation, number of branches appearing on day i, and mean elongation of branches on day i.

Elongation of taproot and branches

It has been shown recently (Aguirrezabal *et al.*, 1994) that elongation of taproot and individual branches of

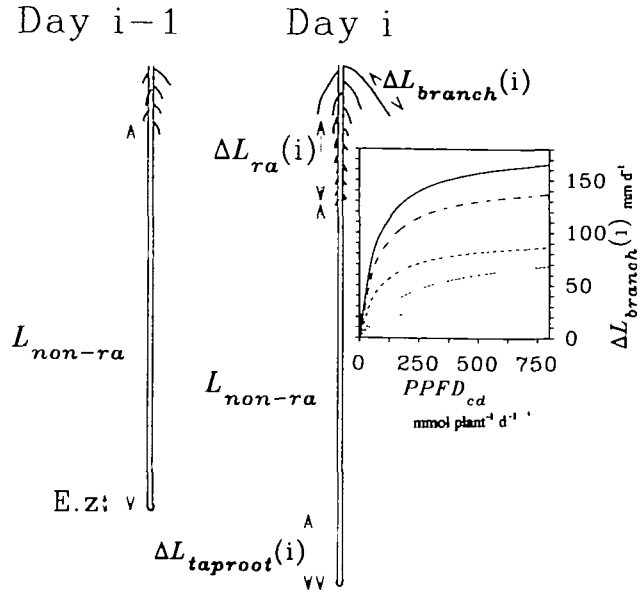

Fig. 1. Representation of variables in architectural analysis. $\Delta L_{taproot}$(i), ΔL_{branch}(i): taproot and individual branch elongation on day i. ΔL_{ra}(i): length of the zone of the taproot carrying new branches on day i. L_{non-ra}: length of the non-ramified zone of the taproot. E.z. Zone of cell elongation in the taproot. Inset: Root elongation rate, ΔL(i) (mm d^{-1}), as a function of daily intercepted photosynthetic photon flux density, $PPFD_{cd}$, (mmol plant^{-1} d^{-1}). (——) taproot. Branches originating at a distance from the taproot base: (— —) from 0–0.1 m; (---) from 0.1–0.2 m; (- - -) 0.2–0.6 m; (···) from 0.6–1 m. Each line represents a hyperbolic function fitted to experimental data obtained in the field and in the growth chamber (Aguirrezabal *et al.*, 1994).

sunflower is closely linked to the *PPFD* intercepted on the previous day (mmol plant^{-1} d^{-1}, called $PPFD_{cd}$ hereafter). After the 2-leaf stage, i.e. when the contribution of photosynthetic carbon became appreciable in root growth, daily taproot elongation rate ($\Delta L_{taproot}/\Delta t$, ranging from 2 to 135 mm d^{-1} in our data) followed a hyperbolic relationship with $PPFD_{cd}$ (inset Fig. 1, r^2 = 0.62 between observed and fitted data):

$$\Delta L_{taproot}/\Delta t = PPFD_{cd}/(a + PPFD_{cd}) \quad (1)$$

where a is a fitted parameter. For a given $PPFD_{cd}$, the taproot elongated faster than branches, and branches originating near the base of the taproot elongated faster than those originating near the apex. Differences in elongation rate among branches were accounted for by the distance between the branch apex and the base of the taproot. The elongation of a branch was related to $PPFD_{cd}$ with a hyperbolic relationship, and to the reciprocal of the distance from the apex of the branch under study to the base of the taproot (approximation of the source–sink distance). The latter was split into the distance that carbon must travel in the taproot (d_{tr}) and in the branch (d_s).

$$\Delta L_{branch}/\Delta t = [PPFD_{cd}/(\alpha + PPFD_{cd})]/(\beta d_{tr} + \gamma d_s) \quad (2)$$

where α, β and γ are fitted parameters. It is noteworthy

that γ had such a low value that d_s had a low weight in the equation. Distribution of elongation, therefore, essentially depended on the position of branches on the taproot (inset Fig. 1). Changes in soil temperature were not taken into account in eqs 1 and 2, and are considered in the analysis presented here.

Number of new branches appearing on day i

This number (N_{ap}(i), d^{-1}) is the product of the length of the taproot segment carrying newly appeared branches on day i (ΔL_{ra}(i), mm d^{-1}, see Fig. 1), and the number of branches per unit taproot length on this segment ($D(z)$ mm^{-1}, z: position on the taproot)

$$N_{ap}(i) = \Delta L_{ra}(i)\ D(z). \quad (3)$$

Both $D(z)$ and ΔL_{ra}(i) can be influenced by time, intercepted *PPFD* and temperature, so that an analysis of N_{ap}(i) must consider these factors. If the length of the non-ramified zone of the taproot ($L_{non\text{-}ra}$, mm, see Fig. 1) was constant over time and experimental conditions, as frequently assumed (Lungley, 1973; Diggle, 1988; Pagès and Aries, 1988), ΔL_{ra}(i) would be equal to taproot elongation on day i. However, $L_{non\text{-}ra}$ is frequently not constant (Geissbühler, 1953; Pagès and Serra, 1994; Pellerin and Tabourel, 1995), so ΔL_{ra}(i) was calculated (Fig. 1) as the difference between taproot elongation on day i ($\Delta L_{taproot}$(i), mm d^{-1}) and the change in length of the non-ramified zone between days i−1 and i ($\Delta L_{non\text{-}ra}$(i), mm d^{-1}).

$$\Delta L_{ra}(i) = \Delta L_{taproot}(i) - \Delta L_{non\text{-}ra}(i). \quad (4)$$

Equation 4 implies that $L_{non\text{-}ra}$ was considered as a variable, instead of as a parameter in current architectural models. It has been analysed here either in terms of length or in terms of time for a material point to cross it once cells have stopped elongating. Since $L_{non\text{-}ra}$ is considerably longer than the length of the elongating zone (*c.* 300 versus *c.* 10 mm), the flux of material points through the non-ramified zone (mm d^{-1}) can be considered as equal to the taproot elongation rate. The time for a material point to cross the non-ramified zone can, therefore, be calculated as the ratio of the length of the non-ramified zone to the taproot elongation rate.

$$t = L_{non\text{-}ra}/(\Delta L_{taproot}/\Delta t) \quad (5)$$

if t (d) is the time for crossing the non-ramified zone, $L_{non\text{-}ra}$ (mm) is the mean length of the non-ramified zone during the timestep under study (one or several days), and $\Delta L_{taproot}/\Delta t$ (mm d^{-1}) is the mean taproot elongation rate during this timestep.

Proportion of branches which stop elongating

In contrast with Lungley's assumptions, it was not considered *a priori* that all branches will elongate. Elongation of the root system on day i was, therefore, analysed as the sum of individual elongations of each apex, multiplied by the probability of this apex continuing to elongate on day i:

$$\Delta L_{root\ system}/\Delta t = \Delta L_{taproot}/\Delta t + \sum[(\Delta L_{branch}/\Delta t) \times (1 - P(i)] \quad (6)$$

if P(i) is the probability for the apex to stop elongating on day i. P(i) has been analysed as a function of time, under contrasting conditions of soil temperature and intercepted *PPFD*.

Materials and methods

Field experiment

Helianthus annuus L. (hybrid 'Ludo') was grown at Grignon, near Paris, in a field with deep clay–loam soil. The detailed characteristics of the experimental design are given elsewhere (Aguirrezabal *et al.*, 1994). Seeds were sown on 24 May, 27 July and 6 September (experiments referred to as SD1, SD2 and SD3 hereafter), in order to get a wide range of soil temperature and *PPFD*. The growing period under study extended from germination to the time when the 10th leaf reached 40 mm in length (called '10 leaf stage' hereafter). This corresponded to 48, 24 and 49 d after sowing in SD1, SD2 and SD3, respectively. A series of seeds was placed in the soil at 35 mm from windows through which root elongation was recorded (no. of windows: 8, 10 and 6 in SD1, SD2 and SD3, respectively). Windows were 2 m wide, 5 mm thick, and either 0.6 or 1 m deep, with an angle to the vertical of 20°. They were covered with 50 mm thick expanded polystyrene sheets in order to prevent light and heat from reaching the roots. The whole trench was also covered with a structure of wood and expanded polystyrene. Shade structures (3 m long × 3 m wide × 1 m high) were placed above half of the plants under study on the 18th, 4th and 17th d after sowing in SD1, SD2 and SD3, respectively, and then moved on the 35th, 17th and 35th d towards the remaining plants. *PPFD* below shade structures ranged from 49–57% of incident *PPFD*. Soil was fertilized after sowing, and watered whenever its water potential, measured every 2nd day with tensiometers placed at 0.6 m from windows at 0.20 and 0.40 m depths, declined below −25 kPa. Soil water potential at 0.6 and 1 m depths remained in the same range of values.

Temperatures were recorded by using thermocouples placed in the soil immediately behind the window at depths of 0.07, 0.15, 0.40, 0.60, and 1 m. Temperature of undisturbed soil (0.40 m depth, 2 m from the windows), air temperature at 0.40 m above the soil and inside the trench were also recorded using thermocouples. Daily mean air temperature (Fig. 2) was higher in SD2 (20.8 ± 2.6 °C) than in SD1 (16.4 ± 3.5 °C), SD3 being still cooler (14.0 ± 4 °C). It tended to increase from germination to the 10-leaf stage in SD1 (Fig. 2), to decrease in SD3 and showed no trend in SD2. Soil temperatures at 0.07 and 0.4 m depths were close to that in the air, with smaller day-to-day variability. It was consistently cooler at lower depths in SD1 and SD2 (Fig. 2b, inset), with still smaller day-to-day variability. Conversely, soil temperature in SD3 at depths greater than 0.4 m decreased more slowly than air temperature, due to heat storage, and was then higher than air temperature. Soil temperature near the windows was close to that in the undisturbed soil in SD1, SD2 and SD3 (mean difference: 0.1, 0.2 and 0.1 °C, maximum difference: 1.4, 2.0 and 2.2 °C). Soil

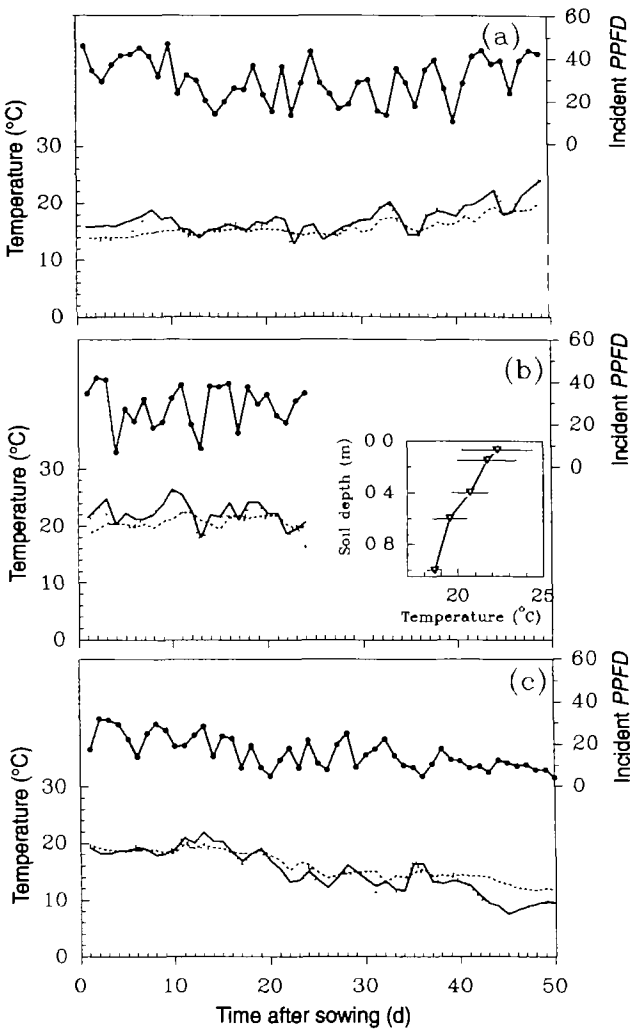

Fig. 2. Mean air and soil temperatures and daily incident photosynthetic photon flux density (incident *PPFD*, mol $m^{-2} d^{-1}$) during the three growing periods in the field, calculated on a daily basis. Sowing dates: (a) 24 May (SD1), (b) 27 July (SD2), (c) 6 September (SD3). (···) Air temperature. (—) Temperature in the soil immediately behind the window at 0.07 m depth. (---) Temperature in the soil immediately behind the window at 0.40 m depth. Inset in (b): Profile of soil temperatures recorded in SD2 on day 19. Horizontal bars: standard errors of the means.

temperature near non-shaded windows exceeded that in shaded windows by 1.0 °C at the 0.07 m depth, 0.7 °C at 0.40 m depth. The temperature experienced by an apex was calculated each day by taking into account the vertical position of this apex and interpolating temperatures measured by thermocouples located above and below the apex under study.

Daily incident *PPFD* (mol $m^{-2} d^{-1}$ was calculated by cumulating over 24 h the recorded values higher than 50 μmol $m^{-2} s^{-1}$. It was higher in SD1 and SD2 than in SD3, with high day-to-day variability during each growing period. The length and width of all the leaves longer than 40 mm was measured and transformed (Pouzet and Bougat, 1985) into leaf area. Intercepted *PPFD* (mmol $plant^{-1} s^{-1}$) was calculated as the product of the mean leaf area per plant and incident *PPFD*, therefore not taking into account self-shading. This is consistent with the fact that, during the period under study when leaf area was small, plant net photosynthesis was linearly related to incident *PPFD* regardless of leaf area and phenological stage (Aguirrezabal *et al.*, 1994).

Taproot and branches were traced every day at 12.00 ± 1 h (solar time) on a transparent plastic sheet placed on the window. A different colour was used every day, so root appearance and elongation corresponding to each day could be recorded.

Daily elongation of roots was measured on the sheets using a rotating wheel and was corrected by taking into account the difference between 12.00 h and the time of measurement. Data taken into account in further calculations are those corresponding to roots which were not in the process of stopping elongation (see eq. 6), thus elongating on the following day.

The number of new branches (length > 10 mm) appearing on day i was counted on plastic sheets. (a) Branch number per unit taproot length, $D(z)$, was counted in each 50 mm section of the taproot. (b) The length of the taproot segment carrying new branches on day i ($\Delta L_{ra}(i)$) was calculated as the difference between the lengths of taproot segments carrying branches on days i and i − 1. This direct way of calculation was compared to that calculated using eq. 4. (c) The length of the non-ramified zone of the taproot on day i was measured, from apex to the nearest branch.

The proportion of branches which stopped elongating was calculated in each experiment by measuring on each plant the individual length of roots originating from two 150 mm segments of the taproot, with at least 20 branches.

Field rhizotron experiment

Helianthus annuus L. (hybrid 'Ludo') was sown in 600 × 450 × 450 mm boxes located in a field near Clermont Ferrand (45°N, 03°E). Three seeds per box were sown on 19 July and 17 August (periods referred to as CA1 and CA2 hereafter), and thinned to one plant per box after emergence. Boxes were watered every day with either water or nutrient solution. Air temperature was measured using a thermocouple at 100 mm above the soil, and was 25.2 ± 2.2 and 19.6 ± 2.9 °C on average in CA1 and CA2. Soil temperature was measured at 0.07, 0.15 and 0.4 m depths, and was close to that in the air (mean temperatures at 150 mm depth: 26.1 ± 2.2 °C in CA1 and 20.2 ± 2.6 °C in CA2. Intercepted *PPFD* was calculated in the same way as in the field experiment (incident *PPFD*: 32.5 ± 7.7 and 23.2 ± 13 mol $m^{-2} d^{-1}$ in CA1 and CA2, respectively). This experiment was only used in the present study for evaluating $D(z)$ and the proportion of branches which stopped elongating. The latter was calculated as in the field study.

Growth chamber experiments

Helianthus annuus L. (hybrid 'Ludo') seeds ranging from 80–110 mg were germinated in the dark at 24 °C. Three days after sowing, three groups of 32 seedlings each were transferred into a nutrient solution (Morizet and Mingeau, 1976) maintained at controlled temperature (20 ± 0.5, 16.5 ± 0.5 or 13 ± 0.5 °C), independently of air temperature (20 ± 1 °C). This experiment was carried out with a *PPFD* of 400 μmol $m^{-2} s^{-1}$ for a photoperiod of 14 h. In another experiment, 80 seedlings were transferred individually to 290 mm deep cylindrical pots (1.2 dm^3 volume) filled with nutrient solution. Seedlings were placed in a growth chamber at 24 ± 1 °C with a *PPFD* of either 550 μmol $m^{-2} s^{-1}$ or 275 μmol $m^{-2} s^{-1}$ for a photoperiod of 16 h.

In both experiments, four plants were sampled daily for a period of 12 d. Taproot length was measured together with the length of the longest branch originating from each of three zones of the taproot (0–0.10 m, 0.1–0.2 m and 0.2–0.3 m from the base of the taproot). Branch number per unit taproot

length, $D(z)$, was counted in each 50 mm section of the taproot and the length of the non-ramified zone of the taproot was measured. Leaf area and intercepted *PPFD* were obtained in the same way as in the field experiment.

Results

Effect of temperature on individual root elongation rate

Before the 2-leaf stage, elongation rates of both taproots and branches followed a linear relationship ($r^2=0.61$ and 0.53, respectively) with the temperature of the apex medium (Fig. 3) in the growth chamber experiment. The slope of the relationship was appreciably smaller for branches than for taproots. Similar relationships were observed in the field with, for taproots, a slope similar to that in the growth chamber (insignificant difference) but a higher intercept ($r^2=0.67$), and a near-zero slope for branches ($r^2=0.07$, NS).

After the 2-leaf stage, the correlation between taproot elongation rate and apex temperature was weaker ($r^2=0.30$). Residuals in the regression between taproot elongation rate and $PPFD_{cd}$ (eq. 1) were still weakly related to the apex temperature ($r^2=0.28$). No relationship was observed for branches. The already low effect observed before the 2-leaf stage, therefore, disappeared during later periods.

Appearance rate of branches

The daily appearance rate of branches ranged from 0 to 17 new branches per day. According to the above-mentioned framework, two factors could contribute to this variability, the number of branches per unit taproot length and the length of the taproot segment carrying new branches.

The profile of branch number per unit taproot length ($D(z)$) was remarkably constant in all our experiments (Fig. 4). In all observed profiles, this number was maximum, with some variability, in the 150 mm upper part of the taproot and was stable (*c.* 5 branches per 50 mm) in deeper parts. In spite of appreciable differences in incident *PPFD* and temperature, similar profiles were observed for the three growing periods (SD1, SD2 and SD3). In neither period did shading affect $D(z)$ appreciably. Furthermore, experiments in Clermont Ferrand with different soil and climatic conditions still provided similar profiles of $D(z)$ (Fig. 4d). Finally, and in order to test the constancy of this profile, $D(z)$ was measured in Weaver's (1926) and in Kutschera's (1960) representa-

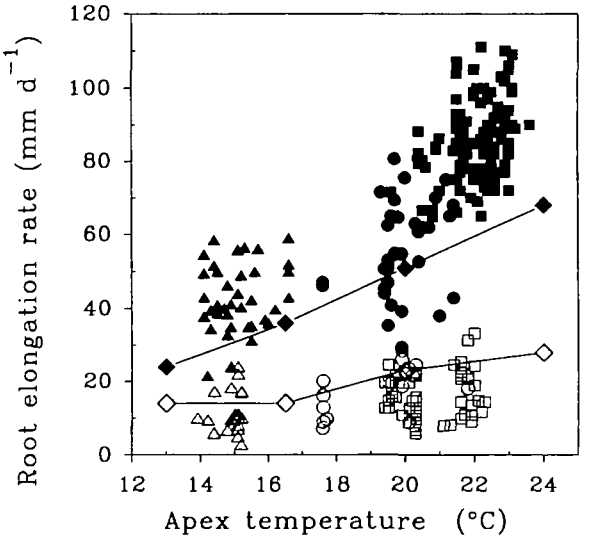

Fig. 3. Root elongation rate (field and growth chamber) as a function of the temperature of the apex medium, from emergence until the 2-leaf stage. These relationships almost disappear later on. Closed symbols: taproot; open symbols: branches. Seedlings were grown in nutrient solution (symbols linked by lines) or in the field (symbols alone). (△): SD1; (□) SD2; (○): SD3.
Equations (field): $\Delta L_{taproot}/\Delta t=6.1\ [T-8.5]$; $\Delta L_{branch}/\Delta t=0.7\ [T-8.5]+4.5$.

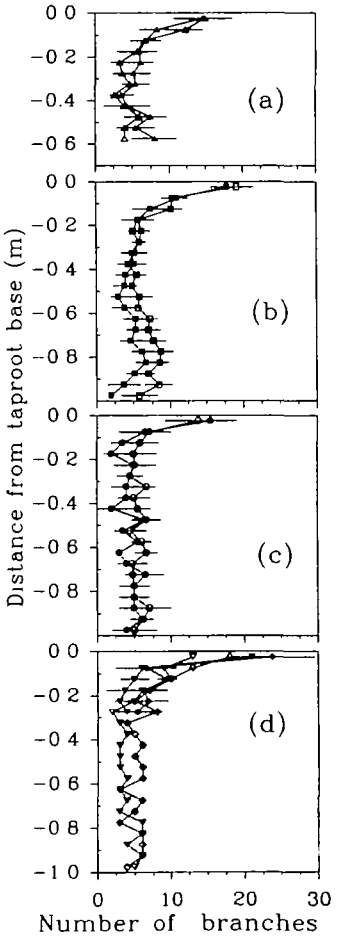

Fig. 4. Profile of branch number per unit taproot length, $D(z)$. (a) SD1, (b) SD2, (c) SD3. Open symbols: non shaded plants; closed symbols: shaded plants. Horizontal bars are standard errors of the means. (d) Profile of branch number per unit taproot length in Clermont Ferrand (CA1, CA2), in Weaver's (1926) and in Kutschera's (1960) representations of sunflower root systems. (▼) CA1; (◆) CA2; (▽) Weaver; (◇) Kutschera.

tions of sunflower root systems. It is interesting to note that $D(z)$ profiles calculated using both authors' data were still very similar to those in our experiments (Fig. 4d).

The length of the taproot segment carrying new branches on a given day varied substantially among days and experiments, and accounted for a great part of the variability in the number of roots appearing on the same day, $N_{ap}(i)$. The relationship between $N_{ap}(i)$ and $\Delta L_{ra}(i)$ ($r^2=0.61$, Fig. 5) was common for plants in SD2 and SD3 (not measured in SD1), and applied for the period from germination to the 2-leaf stage as well as for the period from the 2- to 10-leaf stage. The variability of $\Delta L_{ra}(i)$ was analysed by considering its two components (eq. 4), taproot elongation rate and length of the non-ramified zone on the taproot. $L_{non\text{-}ra}$ appreciably varied among days (3-fold variation), and increased linearly with faster taproot elongation rate (Fig. 6). This relationship was clear in SD2 and in the nutrient solution experiment (Fig. 6a), but variability was greater in SD3. The time for a material point to cross the non-branched zone also changed with taproot elongation rate, calculated times ranging from 3–7 d in 99% of cases.

Combining eq. 4 with the regression equation of $L_{non\text{-}ra}$ as a function of taproot elongation rate allows $\Delta L_{ra}(i)$ to be expressed as a function of $\Delta L_{taproot}(i)$ alone:

$$\Delta L_{ra}(i)=\Delta L_{taproot}(i)-p[\Delta L_{taproot}(i)-\Delta L_{taproot}(i-1)] \quad (7)$$

if p is the slope of the relationship in Fig. 6a. Equation 7 means that $\Delta L_{ra}(i)$ depends on the acceleration of taproot elongation rate. It equals $\Delta L_{taproot}(i)$ if taproot elongation rate does not vary from days $i-1$ to i, while it is smaller (respectively greater) than $\Delta L_{taproot}(i)$ if taproot elongation rate accelerates (respectively decelerates). Prediction of ΔL_{ra} by eq. 7 was good, with a r^2 of 0.82.

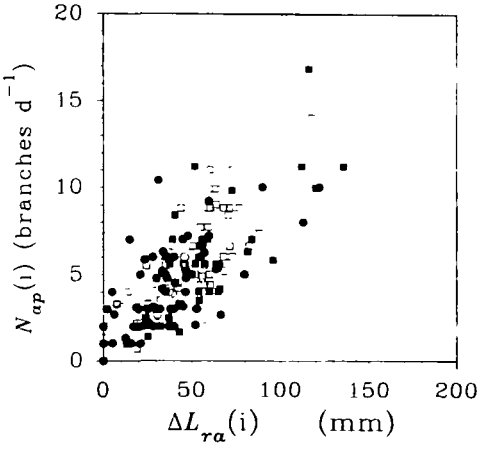

Fig. 5. Daily appearance rate of branches, $N_{ap}(i)$, as a function of the length of the taproot segment carrying new branches, $\Delta L_{ra}(i)$. (□) SD2, (○) SD3. Open symbols: non-shaded plants; closed symbols: shaded plants.

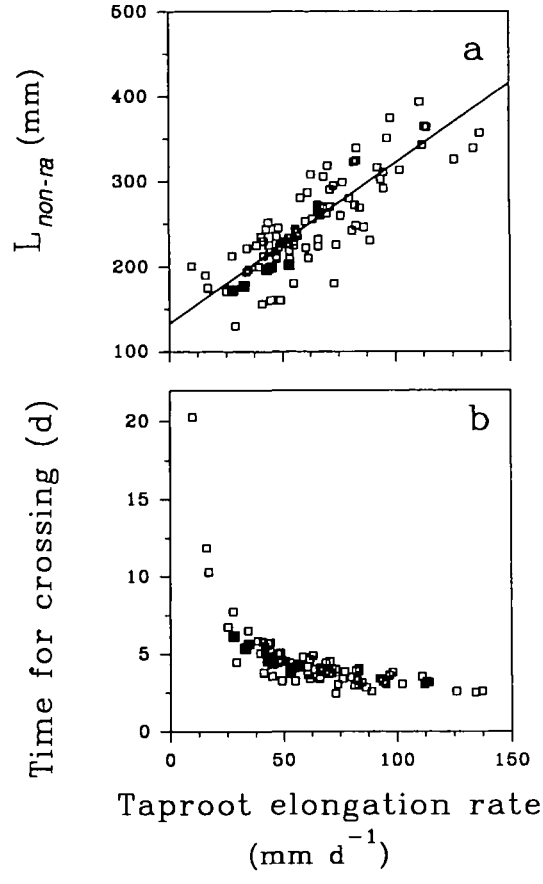

Fig. 6. (a) Length of the non-ramified section of the taproot on a given day ($L_{non\text{-}ra}$) as a function of taproot elongation rate on the same day (b) Time for a material element to cross the non-ramified section of the taproot as a function of taproot elongation rate. (□) Field-grown plants, SD2; (■) Growth chamber experiments. $L_{non\text{-}ra}=132.7+1.9\,\Delta L_{taproot}(i)$.

Proportion of branches which stop elongating

A large proportion of branches stopped elongating at a short distance from the taproot. A quarter of them stopped before reaching 30 mm, less than half reached 50 mm, but most of the branches which elongated for 50 mm reached 150 mm (Fig. 7). This pattern was similar in all experiments, but with markedly different final proportions. Shading did not affect this proportion (Fig. 7a). The only consistent tendency among experiments involved soil temperature (Fig. 7b). The highest proportion of branches which stopped elongating was 83%, observed in SD3 (mean soil temperature during root elongation: 15.6 °C). This proportion decreased with the mean soil temperature during branch elongation (Fig. 7c), with a curvilinear relationship.

Discussion

While current analyses of root growth mainly deal with single root elongation (Sharp *et al.*, 1988; Fraser *et al.*,

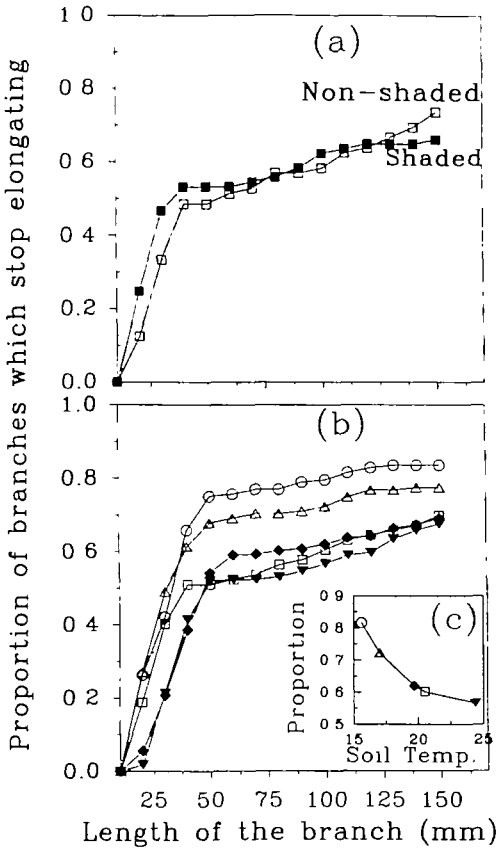

Fig. 7. Proportion of branches which stop elongating, as a function of the length of the branch under study. Curves corresponding (a) to contrasting *PPFD* (shading) and (b) to contrasting growing periods and sites (Grignon and Clermont Ferrand). (a) Open symbols: non-shaded plants; closed symbols: shaded plants (SD2). (b) (△) SD1; (□) SD2; (○) SD3; (▼) CA1; (◆) CA2. (c) Inset: Proportion of branches which have stopped elongating at 100 mm from the taproot, as a function of mean soil temperature.

1990; Pritchard *et al.*, 1990), these results suggest that several other architectural variables could play a crucial role in the variability in elongation of whole root systems linked to environmental conditions.

Effects of intercepted PPFD *and apex temperature on individual root elongation rate*

As discussed in a previous article (Aguirrezabal *et al.*, 1994), the results suggest a major role for intercepted light in the change with time in root elongation rate, and a role for source–sink relationships in the variability in root elongation rate within a root system. These effects are consistent with observed changes in root length due to carbon nutrition (Bingham and Stevenson, 1993; Chaudhuri *et al.*, 1990; Del Castillo *et al.*, 1989; Rogers *et al.*, 1992; Idso and Kimball, 1991, 1992), but they were applied here to day-to-day variability in elongation, and to the variability in elongation within a root system.

In contrast, the role of temperature on root elongation rate was smaller and more complex than expected. As observed by other groups (e.g. Pritchard *et al.*, 1990), apex temperature had an appreciable effect on root elongation rate during the first stages of the plant. This effect was observed in laboratory experiments as well as in the field, but was lower on branches than on the taproot. In the range from 13–24.7 °C, apex temperature had a low direct effect on root elongation rate after the 2-leaf stage. This effect was still detectable, although with very low sensitivity, on taproot elongation rate after the 2-leaf stage, and was not detectable any more on branch elongation. Alternative ways of averaging temperature, by taking into account the temperature in the trench, in undisturbed soil or in the air, also failed to account for the changes in root elongation rate.

Therefore, a model is proposed for individual root elongation which considers two phases. (i) From germination to the 2-leaf stage, when carbon used in root growth predominantly originates from the seed (Aguirrezabal *et al.*, 1994), elongation rate is modelled by taking into account the apex temperature alone (regression equation in Fig. 3). (ii) After the 2-leaf stage, soil temperature had no appreciable effect on branch elongation, neither in growth chamber nor in the field. It is, therefore, proposed that it could be modelled by taking into account intercepted *PPFD* and source–sink distance, and without taking temperature into account (eq. 2). Taproot elongation rate during this second phase was essentially linked to intercepted *PPFD*, with a loose relationship with apex temperature. However, since the residual in the regression of taproot elongation rate was related to apex temperature, it is proposed to combine both effects for modelling:

$$\Delta L_{taproot}/\Delta t = [PPFD_{cd}/(a + PPFD_{cd})]b(T - c) \quad (8)$$

where T is the apex temperature on day i and c is the intercept of the relationship in Fig. 3.

Number of branches

The number of new branches appearing on a given day ranged from near 0 to more than 10 and had, therefore, a considerable effect on total root elongation at the root system level. In our data, it was not linked to the number of branches per unit length of the taproot, $D(z)$, which was surprisingly stable among a wide range of conditions. It was essentially linked to the changes in taproot elongation rate with time or environmental conditions. In contrast with current models of root system architecture (Lungley, 1973; Diggle, 1988; Pagès and Aries, 1988), these data suggest that the apical non-ramified zone of the taproot, $L_{non\text{-}ra}$ can not be considered as having a constant length, consistent with other group's data (Pagès and Serra, 1994; Pellerin and Tabourel, 1995). It can not be considered either to correspond to a constant time of elongation as suggested by Pellerin and Tabourel (1995), since calculated time was negatively related to taproot

elongation rate. An algorithm is proposed, originating from experimental data, where the taproot zone carrying new branches on a given day, $\Delta L_{ra}(i)$, would be equal to taproot elongation rate, plus a term which transiently increases if taproot elongation slows down (eq. 7). The second term in eq. 7 can be substantial if *PPFD* changes between two consecutive days: a change in $PPFD_{cd}$ from 270 to 100 mmol d^{-1} $plant^{-1}$ due to a cloudy day, causing a reduction in taproot elongation rate of 50 mm d^{-1} would eventually increase $\Delta L_{ra}(i)$ and $N_{ap}(i)$ by 45 mm and 4 branches, respectively, instead of decreasing them if the length of the non-ramified zone was considered as constant as frequently assumed. This process could be considered as a buffering mechanism, avoiding brutal changes in the number of new branches. In the longer term, however, taproot elongation rate probably has the greatest contribution in changes in branch appearance.

Proportion of branches which stop elongating

The relatively low proportion of branches which elongate, in relation to appeared branches, might be the main result of this experimental approach. Although this characteristic is usually not taken into account in models, it may be essential since only 20–50% of appeared roots eventually elongate. It has, therefore, a high contribution to the total variability in root length. This characteristic may have an adaptive role. If adverse conditions resulted in a uniform reduction in branch elongation rate, root clumping around the taproot would increase with more adverse conditions. Uptake per unit root length and root water potential would, therefore, decrease, causing earlier stress (Tardieu *et al.*, 1992). In contrast, reducing the number of branches with a smaller effect on the elongation of individual branches reduces clumping and allows higher uptake per unit root length. The knowledge for modelling this proportion is scarce. The absence of effect of shading on this variable is consistent with findings of Del Castillo *et al.* (1989), who observed no change in the number of long roots with CO_2 concentration in the air. The suggestion that it could be linked, at least in part, to soil temperature still needs confirmation and physiological bases.

Overall effects of intercepted PPFD *and of apex temperature*

A model is proposed for root elongation at root system level (Table 1) with a recurrent approach. Taproot elongation rate is first predicted, before the 2-leaf stage, from apex temperature, and after this stage from a combined effect of apex temperature and $PPFD_{cd}$. As the profile of branch density on the taproot did not change in a wide range of conditions, it is proposed to consider it as stable (equation in Fig. 4). The number of branches appearing on day i, therefore, depends on the length of the taproot zone carrying new branches. The latter is related to taproot elongation rate on day i, with a 'buffering capacity' of the length of the non-ramified zone of the taproot (eq. 7). As a consequence, its relationship with environmental variables is indirect, via taproot elongation rate. Branch elongation rate on day i is essentially related to $PPFD_{cd}$, and to the distance between the branch under study and the shoot. The proportion of branches which stop elongating appears to be an essential characteristic for predicting total root elongation. It was linked, in the data, to apex temperature. Although it has not been demonstrated, the amount of carbon available for branch elongation should logically affect this proportion, in order to adjust total branch elongation to carbon supply.

Temperature appears to have a smaller direct effect on root system elongation than that observed by other groups (Klepper *et al.*, 1984; Gregory, 1986; Vincent and Gregory, 1989; Pellerin, 1993). This discrepancy probably has several origins.

—In monocot species, on which the above-mentioned studies were carried out, root axis production is a major

Table 1. *Change with intercepted* PPFD *or apex temperature of the main architectural variables, and bases for modelling*
T, root apex temperature $PPFD_{cd}$, *PPFD* intercepted on the previous day. $\Delta L_{taproot}/\Delta t$, taproot elongation rate. $\Delta L_{ra}(i)$, length of the taproot zone carrying new branches. $L_{non\text{-}ra}$, length of the non-ramified zone. NS, non-significant relationship in the data. *, significant relationship, but low contribution. ***, Essential contribution.

Variable in architectural models	Change with intercepted *PPFD*	Change with apex temperature	Bases for modelling	Equation
Taproot elongation rate				
Before 2-leaf stage	NS	***	Linear relationship with T	In Fig. 2
After 2-leaf stage	***	*	Combined effects of T and $PPFD_{cd}$	Eq. 8
Branch elongation rate	***	NS	Function of $PPFD_{cd}$ and distance to source	Eq. 2
Density of branches on the taproot	NS	NS	Stable	In Fig. 4
Proportion of roots which stop elongating	?	*** (but unsure)	Relationship with T	In Fig. 7
Length of ramified zone of taproot	Indirect, via $\Delta L_{taproot}/\Delta t$		Relationship with $\Delta L_{taproot}/\Delta t$ with buffering capacity of $L_{non\text{-}ra}$	Eq. 7
Number of new branches per day	Indirect, via $\Delta L_{taproot}/\Delta t$		$\Delta L_{ra}(i) \times$ local branch density	Eq. 3

component of root system development and is closely linked to thermal time, while dicot root systems consist of one primary axis only. The production of each new tiller and the production of each new phytomere of a tiller can cause, in monocots, the production of a new generation of root axes. Thermal time, via its effect on both tiller and phytomere productions has, in this case, a crucial effect on the number of growing apices. This effect of temperature does not exist in dicots, where all growing apices originate from the taproot without direct involvement of shoot development.

—Air temperature had, in our data, a crucial *indirect* effect on root elongation on time-scales of weeks, without appreciable direct effect on time-scales of days. It affected leaf appearance rate (Villalobos and Ritchie, 1992) and leaf expansion rate (Rawson and Dunstone, 1986), thereby increasing intercepted *PPFD* and, in turn, root elongation rate. It is, therefore, suggested that the effect of air temperature on root system elongation rate was mainly due to its effect on leaf growth, causing higher light interception.

—The proportion of root which stops elongating had a major contribution to overall root elongation rate, and was linked to temperature in these data. An effect of temperature on elongation rate would have been observed if, in our analysis, all branches had been considered in a single category.

It is argued here that these three indirect effects of temperature at whole-plant level might be at least as important as the effect of temperature on tissue expansion at the root apex level.

Conclusion

These results and their consequences for modelling may seem more complex and less precise than those of previous models. In fact, the objective and approach were different, since experiments, carried out in a wide range of environmental conditions, here preceded modelling. Even if extra complications appeared, it is remarkable that the somewhat simplistic framework proposed by Lungley could hold in the variety of conditions where it was implemented. This is to our knowledge the first attempt to check individually, under field conditions, the hypotheses on which Lungley's model was based, and to relate the parameters of this model to environmental conditions. These data suggest a major role for intercepted *PPFD* on root elongation, and indirectly on branching via taproot elongation. Other apparently obvious mechanisms, such as the effects of temperature on branch density or on individual root elongation rate resulted in having a surprisingly low effect on total elongation. Finally, the proportion of branches which stop elongating after only a few mm might be an essential variable for modelling. A set of equations are given here predicting the effects of changes in intercepted *PPFD* and soil temperature on total root elongation. However, the experimental base is still weak for two crucial processes, namely the change in length of the taproot zone carrying new branches, and the proportion of branches which stop elongating early.

Acknowledgements

We thank Phillippe Hamard (INRA, L.E.P.S.E.) for help in measurements and Bertrand Muller (INRA, L.E.P.S.E.) for reviewing the manuscript. This work was partially supported by CETOM and INTA-INRA convention.

References

Aguirrezábal LAN, Deleens E, Tardieu F. 1994. Root elongation rate is accounted for by intercepted *PPFD* and source sink relations in field and laboratory grown sunflower. *Plant, Cell and Environment* **17,** 443–50.

Bingham LJ, Stevenson EA. 1993. Control of root growth: effects of carbohydrates on the extension, branching and rate of respiration of different fractions of wheat roots. *Physiologia Plantarum* **88,** 149–58.

Chaudhuri UN, Kirkham MB, Kanemasu ET. 1990. Root growth of winter wheat under elevated carbon dioxide and drought. *Crop Science* **30,** 853–7.

Del Castillo D, Acock B, Reddy VR, Acock MC. 1989. Elongation and branching on soybean plants in a carbon dioxide enriched aerial environment. *Agronomy Journal* **81,** 692–5.

Diggle AJ. 1988. ROOTMAP: A model in three-dimensional coordinates of the growth and structure of fibrous root systems. *Plant and Soil* **105,** 169–78.

Fraser TE, Silk WK, Rost TL. 1990. Effects of low water potential on cortical cell length in growing regions of maize roots. *Plant Physiology* **93,** 648–51.

Gandar PW. 1980. The analysis of growth and cell production in root apices. *Botanical Gazette* **14,** 131–8.

Geissbühler H. 1953. Untersuchungen über die korrelative und hormonale Steuerung der Seitenwurzelbildung. *Bericht der Schweizerischen botanischen Gesellschaft* **63,** 27–89.

Gregory PJ. 1986. Response to temperature in a stand of pearl millet (*Pennisetum typhoides*). III. Root growth. *Journal of Experimental Botany* **37,** 379–88.

Idso SB, Kimball BA. 1991. Effects of two and a half years of atmospheric CO_2 enrichment on the root density distribution of three-year-old sour orange trees. *Agricultural and Forest Meteorology* **55,** 345–9.

Idso SB, Kimball BA. 1992. Seasonal fine-root biomass development of sour orange trees grown in atmospheres of ambient and elevated CO_2 concentration *Plant, Cell and Environment* **15,** 337–41.

Klepper B, Belford RK, Rickman RW. 1984. Root and shoot development in winter wheat. *Agronomy Journal* **76,** 117–22.

Kutschera L. 1960. *Wurzelatlasmitteleuropäischer Ackerunkräuter und Kulturpflanzen.* Frankfurt am Main: DLG-Verlags-GmbH.

Lungley DR. 1973. The growth of root systems. A numerical computer simulation model. *Plant and Soil* **38,** 145–59.

Morizet J, Mingeau M. 1976. Influence des facteurs du milieu sur l'absortion hydrique. Etude effectuée sur tomate décapitée en exsudation. *Annales agronomiques* **27,** 183–205.

Pagès L, Aries F. 1988. SARAH: modèle de simulation de la

croissance, du développement et de l'architecture des systèmes racinaires. *Agronomie* **8,** 889–96.

Pagès L, Serra V. 1994. Growth and branching of the taproot of young oak trees—a dynamic study. *Journal of Experimental Botany* **45,** 1327–34.

Pellerin S. 1993. Rate of differentiation and emergence of nodal maize roots. *Plant and Soil* **148,** 155–61.

Pellerin S, Tabourel F. 1995. The length of the apical unbranched zone of maize axile roots: its relationship to the root elongation rate. *Environmental and Experimental Botany* **35,** 193–200.

Porter JR, Klepper B, Belford RK. 1986. A model (WHTROOT) which synchronizes root growth and development for winter wheat. *Plant and Soil* **92,** 133–45.

Pouzet A, Bougat F. 1985. Description d'une méthode simple et rapide pour l'estimation de la surface foliaire de la plante chez le tournesol. *Proceedings XI Sunflower International Conference, Mar del Plata (Argentine),* 21–3.

Pritchard J, Barlow PW, Adam JS, Tomos AD. 1990. Biophysics of the inhibition of the growth of maize roots by lowered temperature. *Plant Physiology* **93,** 222–30.

Rawson HM, Dunstone RL. 1986. Simple relationships describing the responses of leaf growth to temperature and radiation in sunflower. *Australian Journal of Plant Physiology* **13,** 321–7.

Ritchie JT, Otter S. 1984. *CERES-Wheat: a user-oriented wheat yield model.* Preliminary documentation, AGRISTARS Publication No YM-U3-04442-JSC-18892.

Rogers HH, Peterson CM, McCrimmon JN, Cure JD. 1992. Response of plant roots to elevated atmospheric carbon dioxide. *Plant, Cell and Environment* **15,** 749–52.

Silk WK. 1992. Steady form from changing cells. *International Journal of Plant Science* **153,** S49–S58.

Sharp RE, Silk WK, Hsiao TC. 1988. Growth of the maize primary root at low water potentials. I. Spatial distribution of expansive growth. *Plant Physiology* **87,** 50–7.

Tardieu F, Bruckler L, Lafolie F. 1992. Root clumping may affect the root water potential and the resistance to soil–root water transport. *Plant and Soil* **140,** 291–301.

Villalobos FJ, Ritchie JT. 1992. The effect of temperature on leaf emergence rates of sunflower genotypes. *Field Crops Research* **29,** 37–46.

Vincent CD, Gregory PJ. 1989. Effects of temperature on the development and growth of winter wheat roots. I. Controlled glasshouse studies of temperature, nitrogen and irradiance. *Plant and Soil* **119,** 87–97.

Weaver JE. 1926. *Root development of field crops.* New York: McGraw Hill.

Williams JR, Jones CA, Dyke PT. 1984. A modelling approach to determining the relations between erosion and soil productivity. *Transactions of the ASAE* 129–44.

Williams JR, Jones CA, Kiniry JR, Spanel DA. 1989. The EPIC crop growth model. *Transactions of the ASAE* 497–511.